Ultrasonics xxx (xxxx) xxx–xxx

Contents lists available at ScienceDirect

Ultrasonics

journal homepage: www.elsevier.com/locate/ultras

Fundamental wave amplitude difference imaging for detection and characterization of embedded cracks

Sylvain Haupert[a,*], Yoshikazu Ohara[b], Ewen Carcreff[c], Guillaume Renaud[a]

[a] Sorbonne Université, CNRS UMR 7371, INSERM UMR S 1146, Laboratoire d'Imagerie Biomédicale, Paris, France
[b] Department of Materials Processing, Graduate School of Engineering, Tohoku University, 6-6-02 Aoba, Aramaki-aza, Aoba-ku, Sendai 980-8579, Japan
[c] The Phased Array Company, 8 bis rue de la garde, 44300 Nantes, France

ARTICLE INFO

Keywords:
Ultrasonic imaging
Amplitude modulation
Phased array
Nonlinear scatterers
Fatigue crack
Thermal crack
Fundamental wave amplitude difference (FAD)
Fundamental amplitude subtraction

ABSTRACT

An ultrasonic technique for imaging nonlinear scatterers, such as partially-closed cracks, buried in a medium has been recently proposed. The method called fundamental wave amplitude difference (FAD) consists of a sequence of acquisitions with different subsets of elements for each line of the image. An image revealing nonlinear scatterers in the medium is reconstructed line by line by subtracting the responses measured with the subsets of elements from the response obtained with all elements transmitting. In order to get a better insight of the capabilities of FAD, two metallic samples having a fatigue or thermal crack are inspected by translating the probe with ultrasonic beam perpendicular (i.e. parallel) to the crack direction which is the most (i.e. less) favorable case. Each time, the responses of the linear scatterers (i.e. conventional image) and nonlinear scatterers (i.e. FAD image) are compared in term of intensity and spatial repartition. FAD exhibits higher detection specificity of the crack with a better contrast than conventional ultrasound imaging. Moreover, we observe that both methods give complementary results as nonlinear and linear scatterers are mostly not co-localized. In addition, we show experimentally that FAD resolution in elevation and lateral follows the same rule as the theoretical resolution of conventional ultrasonic technique. Finally, we report that FAD gives the possibility to perform parametric studies which let the opportunity to address the physical mechanisms causing the distortion of the signal. FAD is a promising and reliable tool which can be directly implemented on a conventional open scanner ultrasound device for real-time imaging. This might contribute to its fast and wide spread in the industry.

1. Introduction

Early detection and sizing of cracks embedded in a material is crucial to ensure the safety of strategic structures such as oil pipelines, railway tracks, wings of aircraft or pipelines in nuclear power plants. The industrials need fast and reliable techniques that could be easily deployed in the field. If cracks are completely open, they can be accurately measured by conventional ultrasonic testing (UT), i.e. linear ultrasonics, since ultrasound is strongly scattered at the crack tip. However, some fatigue cracks are partially-closed due to the mechanisms of plasticity, roughness, or oxide-induced crack closure [1]. Closed parts of the cracks can be underestimated or overlooked by conventional UT, since no echoes are generated [2]. Conventional UT is blind to these specific features. On the contrary, it is now well established that nonlinear ultrasonics are very sensitive to micro-damage such as partially-closed cracks [3–5]. Nonlinear ultrasonics is generally based on the detection of nonlinear components, e.g. superharmonic waves ($2f$, $3f$…) or subharmonic waves ($f/2$, $f/3$,…), which are generated due to the nonlinear interaction between ultrasound and defects. This has been referred to as contact acoustic nonlinearity (CAN) [6]. Until about 10 years ago, the studies of nonlinear ultrasonics had been mainly based on waveform analyses received by monolithic transducers [7] making difficult rapid 3-D scan of specimen. Recently, new nonlinear imaging techniques based on phased arrays have been proposed to image with high sensitivity buried partially-closed cracks that remain mostly invisible to conventional imaging [8–13].

This paper contributes to the characterization of the so-called fundamental wave amplitude difference (FAD) technique, which is one of the imaging methods based on the fundamental wave amplitude dependence [10] of nonlinear response. A detailed comparison between FAD and earlier similar methods can be found in [11]. FAD is a practical technique in terms of imaging speed and equipment cost which

* Corresponding author.
E-mail address: sylvain.haupert@upmc.fr (S. Haupert).

https://doi.org/10.1016/j.ultras.2019.02.003
Received 13 June 2018; Received in revised form 1 February 2019; Accepted 4 February 2019

might contribute to its fast and wide spread in the industry. In order to have a better understanding of the capabilities of FAD, two samples, one with a mechanical fatigue crack [8,14,15] and the other one with a thermal fatigue crack [11] are inspected. Each time, the responses of the linear scatterers (i.e. conventional image) and nonlinear scatterers (i.e. FAD image) are compared in term of intensity and spatial repartition. We also compare the ability of FAD technique to distinguish the crack from the rest of the sample by performing images across the crack (i.e. the ultrasonic beam is perpendicular to the crack direction which is the most favorable case) and/or along the crack (i.e. the ultrasonic beam is parallel to the crack direction which is the less favorable case). Then FAD resolution in elevation and lateral direction is evaluated experimentally and compared to the theoretical resolution of conventional UT. Finally, we show that FAD technique gives the possibility to perform parametric studies which opens the opportunity to address physical mechanism causing the distortion of the signal.

2. Material and methods

2.1. Fundamental amplitude difference (FAD) imaging technique

FAD is described in details in a previous paper [11]. Briefly, we recall that FAD is based on the amplitude dependency of the distortion of an incident ultrasonic wave caused by non-linear scatterers by opposition to the conventional linear ones. Linear scatterers are holes, grains or slits that backscatter the incident wave whereas non-linear scatterers are micro-damages such as flaws, microcracks, partially-closed crack or dislocations which behave as non-linear elastic sources due to clapping, slipping or friction at micro or nano contacts level [16]. It follows that part of the incident ultrasonic wave is distorted, changing its frequency content by adding sub-harmonics and/or super-harmonics, decreasing the amplitude of the fundamental frequency. Moreover, this phenomenon is amplitude dependent meaning that the response of the nonlinear scatterers is not proportional to the incident ultrasonic wave amplitude.

The simplest FAD configuration consists of a sequence of three acquisitions for each line of the image. It has been implemented with conventional phased array transducers. The first acquisition is obtained by transmitting with all elements of the phased array transducer while the second and third acquisitions are obtained by transmitting with odd elements only and even elements only, respectively. Before processing data, each signal is filtered around the fundamental frequency. Then, an image revealing nonlinear scattering in the medium is reconstructed line by line by subtracting the responses measured with second and third acquisitions (odd elements and even elements) from the response obtained with all elements transmitting. Indeed, the response of the nonlinear scatterers is expected to be not proportional to the amplitude. In addition to the FAD image, a conventional (i.e. linear) image is reconstructed for comparisons from the data acquired with all elements transmitted, using the conventional delay-and-sum technique.

Data acquisition, processing and image reconstruction were performed on Matlab R2017a (Mathworks, Natick, Massachusetts, USA).

2.2. Thermal fatigue crack experimental setup

The first sample is a stainless steel AISI304 parallelepiped sample ($61 * 150 * 100\ mm^3$), the same that was used in the previous paper [11]. It has a small buried crack produced *in-situ* by controlled thermal fatigue loading (Trueflaw Ltd, Espoo Finland). Trueflaw claims the process creates realistic simulation of mechanical and thermal fatigue cracks and good simulation of stress corrosion cracks [17]. The apparent 24.2 mm length of the crack (i.e. *y*-direction) was optically measured at the surface of the sample by dye penetrant inspection while the 5.9 mm depth of the crack (i.e. *z*-direction) was estimated, not measured, by the manufacturer. The plane of the crack is approximately in plane *y*-*z* (see Fig. 1). The longitudinal wave velocity in the sample is assumed to be 5700 m/s.

The measurements are done with a 5 MHz linear array (64 elements – pitch of 1 mm – Imasonics, Voray sur l'Ognon, France) coupled to an open ultrasonic scanner OEM-PA system (output voltage 145 Vpp – Advanced OEM Solutions, Cincinnati, USA). The phased array is positioned on the top of the sample on the opposite side to the crack (i.e. bottom part). A coupling gel is used to promote ultrasound transmission penetration inside the sample. Two scans are performed by translating manually the probe: (1) along the crack (i.e. translation in *y*-direction by step $\Delta y = 1$ mm); the probe is positioned centrally over the crack, perpendicular to the plane of the crack) and (2) across the crack (i.e. translation in x-direction by step $\Delta x = 1$ mm); the probe is in same plane *y*-*z* as the crack plane), see Fig. 1. Thirty 1 mm-steps (i.e. corresponding to 1/5 of the elevation width of the probe) are needed to scan the entire crack. For each position, fixed focusing is performed in transmission and reception at $\Delta z = 57$ mm in depth (i.e. direction *z*; where the crack tip is expected) and by beam-steering in plane *x*-*z* (i.e. perpendicular scan) or in plane *y*-*z* (i.e. parallel scan) from -15 mm to 15 mm with an electronic step $\Delta e = 250$ µm. FAD and conventional images are reconstructed from the same data set.

Sixteen acquisitions are performed at each position and averaged to achieve high signal-to-noise ratio level. Finally, different ratios are tested: ratio 2 (i.e. full aperture: 64 elements, then 2 sub-apertures: 2×32 elements), ratio 4 (i.e. 64 elements, then 4×16 elements), ratio 8 (i.e. 64 elements, then 8×8 elements), ratio 16 (i.e. 64 elements, then 16×4 elements). Sub-apertures involve different elements without repetition.

2.3. Mechanical fatigue crack experimental setup

The second sample is an aluminum alloy A7075 parallelepiped sample ($30 * 40 * 170\ mm^3$) that was already measured in several previous papers [8,14,15]. It has a mechanical fatigue crack that was initiated from a notch on a three-point bending fatigue test with a maximum stress intensity factor of $4.3\ MPa{\cdot}m^{1/2}$ and a minimum stress intensity factor of $0.6\ MPa{\cdot}m^{1/2}$. The depth from the bottom on the side surfaces was optically measured to approximately 20 mm, which corresponds to the half of the thickness. The longitudinal wave velocity in the sample is assumed to be 6300 m/s.

The measurements are done with another 5 MHz linear phased array (128 elements – pitch of 0.5 mm – Imasonics, Voray sur l'Ognon, France) coupled to an open ultrasonic scanner OEM-PA system (output voltage 145 Vpp – Advanced OEM Solutions, Cincinnati, USA). A sub-aperture of 64 elements, from element #9 to element #72 are chosen to avoid using broken elements and reducing the amount of energy deliver in the material. The phased array is positioned on the top of the sample on the opposite side to the crack (i.e. bottom part) as for the aluminum alloy specimen. The probe is oriented in the plane *x*-*z*, perpendicular to the crack plane (i.e. plane *y*-*z*). A scan is performed by translating manually the probe along the crack (i.e. in y- direction), see Fig. 2. Sixteen 1 mm-steps (i.e. corresponding to 1/10 of the elevation width of the probe) are needed to scan the entire crack. For each position, both conventional and FAD images are obtained by focusing the ultrasound beam at 20 mm in depth (i.e. direction *z*; where the crack tip is expected) and by beam-steering (i.e. in plane *x*-*z*) from -25 mm (i.e. $\theta = 51°$) to -5 mm (i.e. $\theta = 15°$) with an electronic step $\Delta e = 750$ µm. This time, the reconstruction involves continuous dynamic-receive beamforming during the delay-and-sum process.

Sixty four acquisitions are performed with a ratio of 2 (i.e. full aperture, then odd and even elements) at each position and averaged to achieve high signal-to-noise ratio level. A coupling gel is used to promote ultrasound transmission penetration inside the sample.

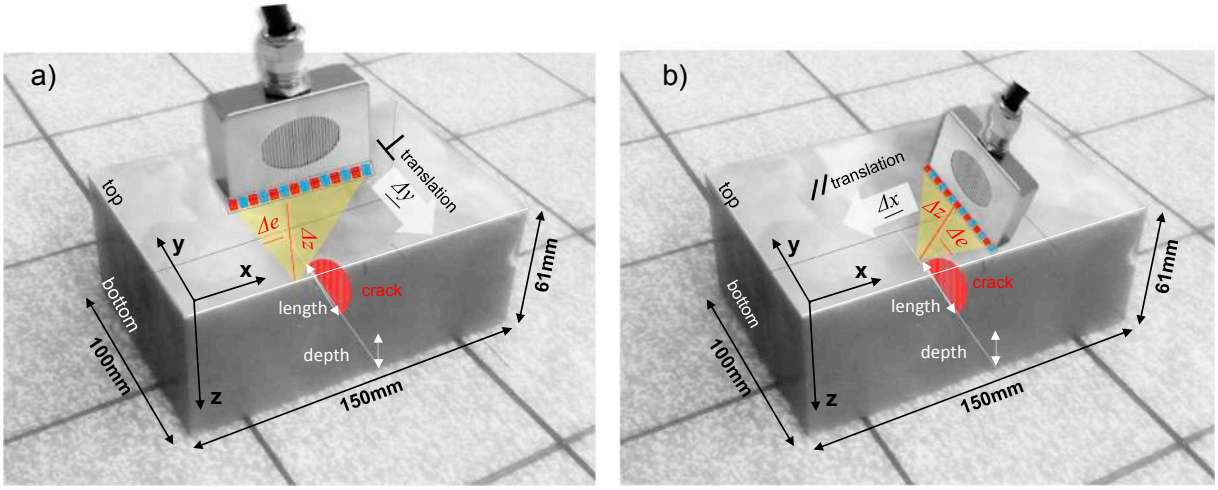

Fig. 1. Schematic of the stainless steel specimen with the position of the phase-array and both configurations: (a) perpendicular translation (i.e. translation along *y*-direction with beam steering in the plane *x*-*z*) and (b) parallel translation (i.e. translation along *x*-direction with beam steering in the plane *y*-*z*). The plane of the crack is *y*-*z*.

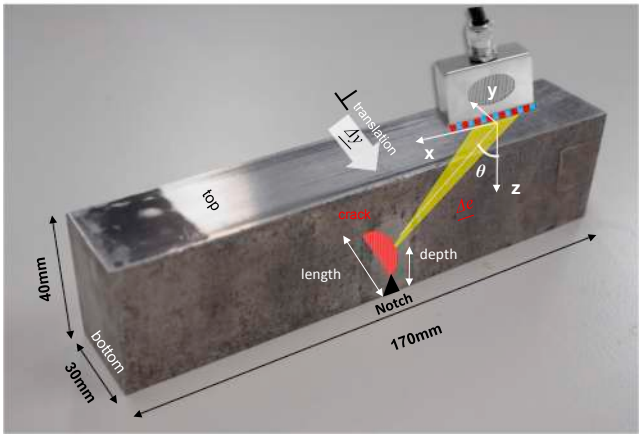

Fig. 2. Schematic of the aluminum-alloy specimen with the position of the phase-array as well as the electronic beam-steering.

3. Results and discussion

3.1. Thermal fatigue crack specimen results

After acquisitions, conventional and FAD images are reconstructed using the same data set. To compare both results, images are plotted in dB scale, where 0 dB is defined as the maximum amplitude signal in the conventional image, i.e. the echo from the back wall. If there is no mention of the ratio, data obtained with ratio 2 are displayed and analyzed.

Two sets of images obtained for different orientation of the probe are shown for a better sake of clarity in Figs. 3 and 4. They correspond to positions where the contrast is the highest for both methods. The position of the probe is respectively the twentieth translation step parallel (i.e. *y*-direction) to the crack plane (i.e. *y*-*z* plane) and the thirteen translation step perpendicular (i.e. *x*-direction) to the crack plane (i.e. *y*-*z* plane). This explains why the crack shape is totally different in both figures. Outside the crack location, the background pattern is different for the conventional and FAD methods. In case of the conventional method, a structural noise due to grains speckle is clearly visible. Regarding FAD, the noise pattern does not look like speckle but sparse spikes, due to fast low thermal and/or electronic fluctuations. Apart from this noise, a strong residue with a level of −36 dB should be noticed in the nonlinear image. It appears at the back wall is an artefact of FAD. Of course, the back wall of the specimen is strictly a linear scatterer and cannot produce nonlinear signal. Actually, this residue corresponds to the remaining of a signal created by linear scatterer that is not completely canceled after applying FAD due to inter-elements coupling of the phased array [11]. Thus, the best reduction that can be done with this experimental setup is a 36 dB reduction of the linear signal at the back wall but also at the crack position. Very recently, a method similar to FAD has been suggested to reduce this artefact [13]. This remark might raise the crucial question about the interpretation of the origin of the signal obtained by FAD in the rest of the image, especially at the positions of strong signals. Is it strictly a manifestation of nonlinear elastic mechanisms or a residue of the linear scattering? This question can be answered by comparing the ratio (i.e. difference in case of dB) of the linear and nonlinear signals at the very same position. If the nonlinear signal is much higher than the linear signal minus 36 dB, then the origin of the signal measured by FAD is strictly nonlinear. For instance, in Figs. 3 and 4 the maximum found in the conventional image is −37 dB while it is respectively −43 dB in the FAD image at the very same position, which is much higher than the expected linear residue (i.e. −37 dB − 36 dB = −73 dB) in case of absence of nonlinear scattering. This comparison can be performed for each nonlinear scatterer measured by FAD, each time, the nonlinear signal is much higher than the linear residue, confirming that FAD does not measure a residue of the linear scattering, neither a mixture of linear and nonlinear scatterers but rather measure strictly nonlinear scatterers.

Finally, the 6 mm crack depth itself can be determine in all images, although it should be noted that it is easier to determine the limit of the crack in FAD than in conventional images. Moreover, it seems that the crack penetration profile is better disentangled from the background noise in the FAD picture as shown in Fig. 4. It should be noticed that for fair comparison, the dynamic is kept constant at 40 dB, with the lowest value equal to the mean background noise level.

In order to appreciate the variation of the pixels value, a graph is displayed on the right side of the images. It corresponds to pixels along the horizontal line (i.e. white line) passing through the highest pixel value in the crack area. These graphs show the background noise and its fluctuation as well as the peak value corresponding to the highest linear and nonlinear signal produce by the crack. The contrast can be evaluated by measuring the difference between the peak value and the mean value of the background. We found that the mean background noise is −82 dB and −57 dB for the FAD and conventional methods respectively while the background noise standard deviation is 5.5 dB for

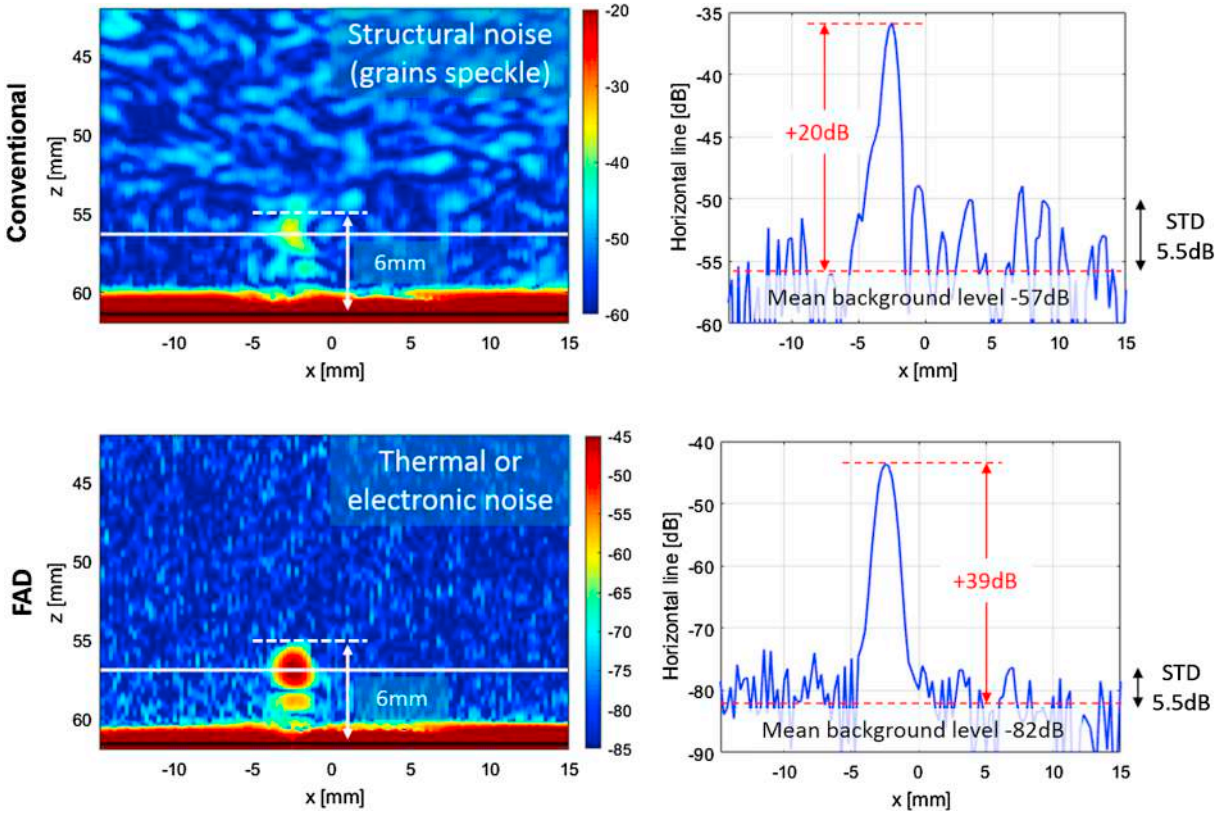

Fig. 3. [Thermal fatigue crack specimen] Contrast and background noise comparison between the conventional (i.e. linear) and the fundamental wave amplitude difference (FAD) (i.e. nonlinear) methods performed with electronic beam steering across the crack direction (i.e. perpendicular scan).

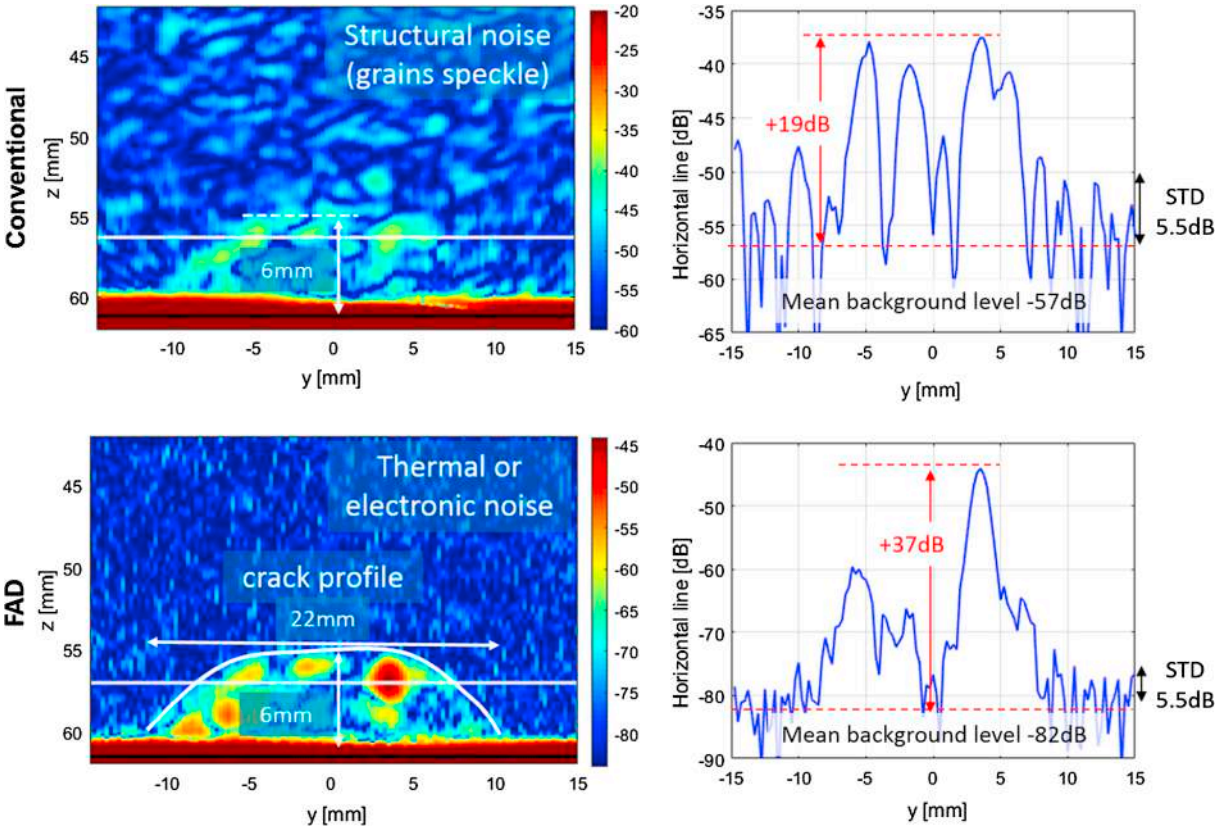

Fig. 4. [Thermal fatigue crack specimen] Contrast and background noise comparison between the conventional (i.e. linear) and the fundamental wave amplitude difference (FAD) (i.e. nonlinear) methods performed with electronic beam steering along the crack direction (i.e. parallel scan).

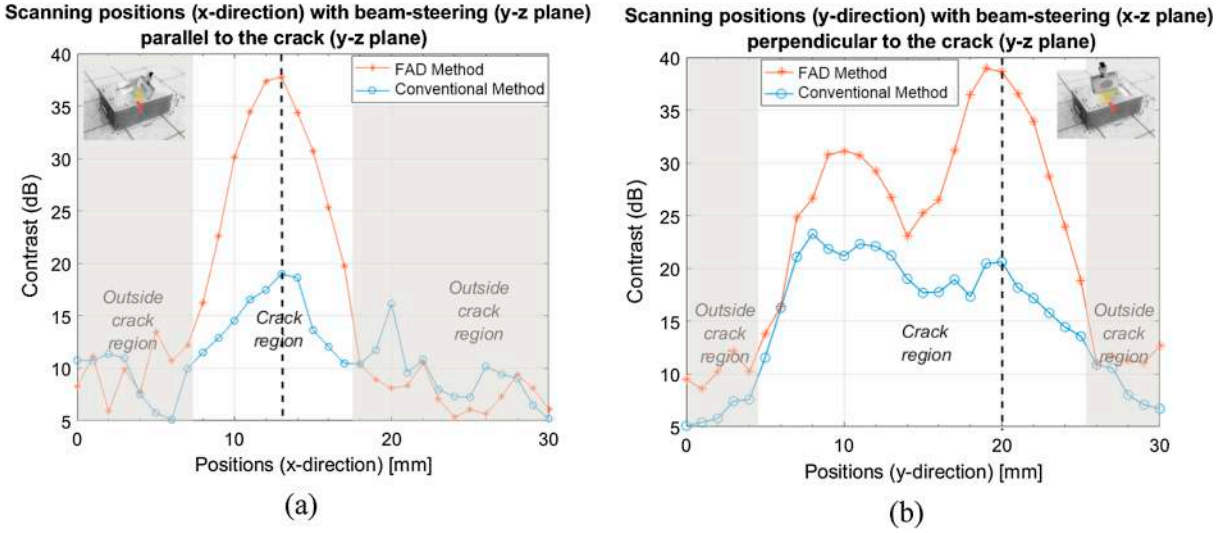

Fig. 5. [Thermal fatigue crack specimen] Contrast comparison between the conventional (i.e. linear) and the fundamental wave amplitude difference (FAD) (i.e. nonlinear) methods performed with a mechanical translation of the probe across (a) or along (b) the crack direction. The vertical black dotline shows the correspondence with Figs. 3 and 4.

both methods. The contrast is calculated for both sets of measurements: slices obtained with beam-steering perpendicular (i.e. *x*-*z* plane) to the crack plane (i.e. *y*-*z* plane) and probe translation along the crack (i.e. in *y*-direction) (Fig. 5a) and slices obtained with beam-steering parallel (i.e. *x*-*z* plane) to the crack plane (i.e. *y*-*z* plane) and translation across the crack (i.e. in *x*-direction) (Fig. 5b). In both cases, the contrast is higher for the FAD method than the conventional method with a maximum contrast of 39 dB in case of FAD compared to 22 dB for the conventional method. Outside the crack region, one can observe a contrast between 5 and 11 dB, i.e. equal to one to two times the value of the standard deviation of the background noise. Vertical black lines show both selected positions displayed in Figs. 3 and 4.

To address the question of FAD resolution, we make the assumption that the thickness of the crack is so small that it can be considered as a point source in the *y*-direction. Lateral resolution is extracted from the nonlinear intensity profile of the most energetic scatterers obtained during scanning perpendicular to the crack direction (see Fig. 6a). Elevation resolution is calculated by aggregating vertical lines passing through the most energetic scatterers located at y = 4 mm (see Fig. 6b) in all thirty 1 mm-step images.

The results show that the lateral resolution is 1.3 mm (i.e. the bandwidth at −6 dB). In theory, for the conventional method, the lateral resolution is 4* λ/π * F-number = 1.27 mm, with the wavelength λ = 1.1 mm and F-number = 0.9. The elevation resolution is 5 mm (i.e. the bandwidth at −6 dB). In theory, for conventional method, the elevation resolution corresponds to the width of the piezo-electric element, i.e. 5 mm for this linear-array with no lens. Finally, axial resolution was not measured as it supposes to bring closer two nonlinear scatterers until it is not possible to distinguish them. Thus, the resolution of the FAD method follows the same rules as the conventional image. This is not surprising as FAD method does not involve harmonics or sub-harmonics but the exact same bandwidth centered at the fundamental frequency of the phased-array.

The last results obtained with the thermal fatigue crack specimen concern the response of the nonlinear scatterers at different amplitudes of excitation. The highest level of excitation is kept constant by using each time all elements of the phased-array (i.e. 64 elements) while the lowest level of excitation varies from half the number of elements (i.e. ratio 2) to one over sixteen of elements (i.e. ratio 16). As the mechanisms involve in the nonlinear response depends by definition on the level of excitation, we expect the amplitude of the FAD signal to depend on the ratio. As we examine the very same area with ratio 2, ratio 4, ratio 8 and ratio 16, it may be possible to extract the FAD signal, also called the nonlinear residue A_{NL}, for each configuration. We choose to pick the value of the most energetic pixel found at the crack location (i.e. the same location as in Figs. 3 and 6(a) for different ratios. In Fig. 7, we observe that the nonlinear residue A_{NL} increases as the ratio increases (i.e. the lowest level of excitation decreases). One can also notice that the increase of A_{NL} is followed by a plateau. These observations could be explained by the fact that in case of ratio 2 and ratio 4, nonlinear scatterers may also have been excited with half or a quarter of elements. As the number of elements decreases, the nonlinear scatterers are less and less excited until a threshold level where no more nonlinear mechanisms are involved as it may appear for ratio 16.

It is tempting to develop a simple nonlinear model based on the hypothesis that the nonlinearity, i.e. the residue A_{NL}, increases as a power law n of the excitation A, with N, the ratio:

$$A_{NL} = A^n - N(A/N)^n \quad (1)$$

A^n is the nonlinear response obtained when using all elements of the phased-array, while $(A/N)^n$ is the nonlinear response obtained with the subset of elements corresponding to the ratio (i.e. N = 2, 4, 8, and 16). The best fit of the experimental data with eq.1 is obtained when n = 1.7. It is difficult to compare with common nonlinear elastic models which are mostly based on the 2nd harmonics considering the amplitude of the fundamental frequency as a constant. For example, in case of the nonlinear elasticity due to lattice anharmonicity [18], the power law follows by the 2nd harmonics is expected to be 2. The same is expected for the bubbles [19]. In case of clapping, the power law is expected to be 3/2 [20,21].

This is the first step towards parametric images of nonlinear elastic phenomena. Indeed, one could think doing this operation for all pixels corresponding to the crack in order to create a parametric image of the power law *n*, expecting different values of *n* depending on the nonlinear elastic behavior of the nonlinear scatterers. Moreover, we need to find a way to compare the results with the existing nonlinear elastic models.

3.2. Mechanical fatigue crack specimen results

Underestimation of the crack depth is a major industrial problem. Recently, the focus is on the mechanical fatigue crack whom part is (partially) closed, meaning that they are invisible to conventional ultrasonic techniques [8,15]. In this part, FAD technique is qualitatively compared to the conventional imaging technique in order to get a better

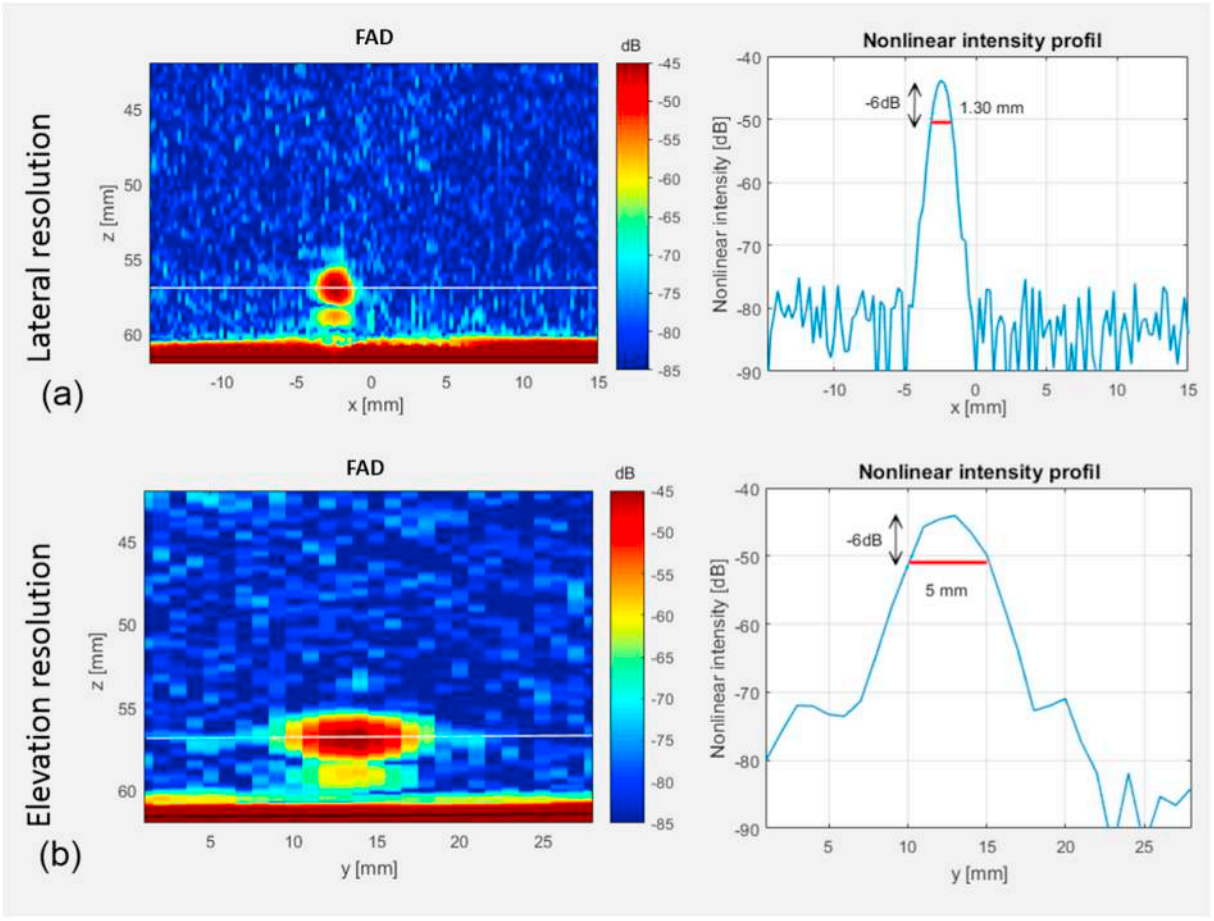

Fig. 6. [Thermal fatigue crack specimen] (a) Lateral and (b) elevation resolutions of FAD method. The resolution of FAD follows the same rules as the conventional linear echographic imaging technique.

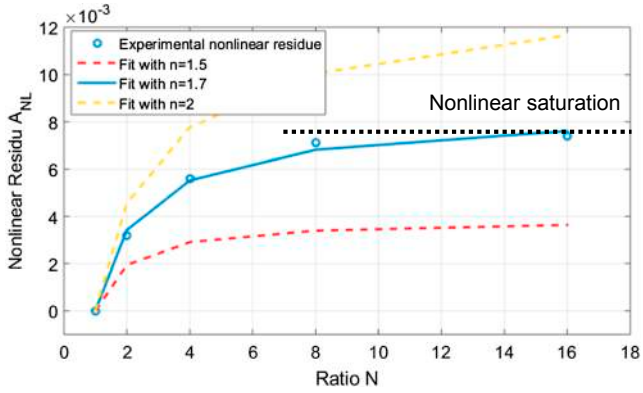

Fig. 7. [Thermal fatigue crack specimen] Contrast and background noise comparison between the conventional (i.e. linear) and the fundamental wave amplitude difference (FAD) (i.e. nonlinear) techniques. Perpendicular scan.

insight if FAD is able to help obtaining a better estimation of depth of partially closed crack.

Normalization of the conventional (i.e. FAD) images is performed by dividing the amplitude of each pixel in the image by the average of the maximum values found in the conventional (i.e. FAD) images among the 16 slices at the crack location (between 12 mm and 25 mm).

A 3D representation of the 16 slices is displayed in Fig. 8 for both methods. The notch is clearly seen in the conventional 3D scan but not in the FAD 3D scan as expected. Indeed, the notch is a strong linear scatterer which cannot behaves nonlinearly (e.g. no clapping neither slipping mechanisms). The positions of the hot spots (i.e. in red color) are different in both 3D scans. At a first glance, linear and nonlinear scatterers' responses seem not being collocated. In order to appreciate their distribution across the crack length, the values upper than 0.5 (i.e. equivalent to -6 dB) are kept for both methods, merged and displayed in different color for all 16 slices (see Fig. 9). Blue color corresponds to the nonlinear response alone, red color corresponds to the linear response alone and yellow color corresponds to the overlapping of linear and nonlinear responses. Images obtained with both methods at 4 characteristic positions (i.e. 0 mm, 6 mm, 7 mm and 16 mm) are displayed for a better sake of clarity. With this representation, we can observe that few linear and nonlinear scatterers seem collocated. This is likely due to the lack of resolution of both techniques, which cannot resolve the position of linear and nonlinear scatterers that are separated by a distance close or smaller than the lateral resolution (i.e. 1.3 mm) or axial resolution. The collocation is mainly in the central part of the crack at positions 7 mm to 10 mm. Linear and nonlinear scatterers are both present all along the crack except at the central position (i.e. 6 mm) and at the end of the crack (i.e. position 15 mm). Finally, the nonlinear response is mainly observed at the crack tip or above the crack tip (i.e. > -20 mm) while the linear response is observed 7, 8 and 9 mm where both linear and nonlinear scatterers are collocated. This mean that both conventional and FAD methods are necessary to have a better estimation of the crack length. Without FAD, we can miss the partially closed part of the crack above the open crack tip.

A side observation which worth to be mentioned is found when the 16 slices are averaged (i.e. equivalent to a projection along *y*-direction) (see Fig. 10). First, we can observe that the maximal values are not localized at the same position, the nonlinear scatterers' response is higher than the linear. It confirms what we observe in Fig. 9. The most

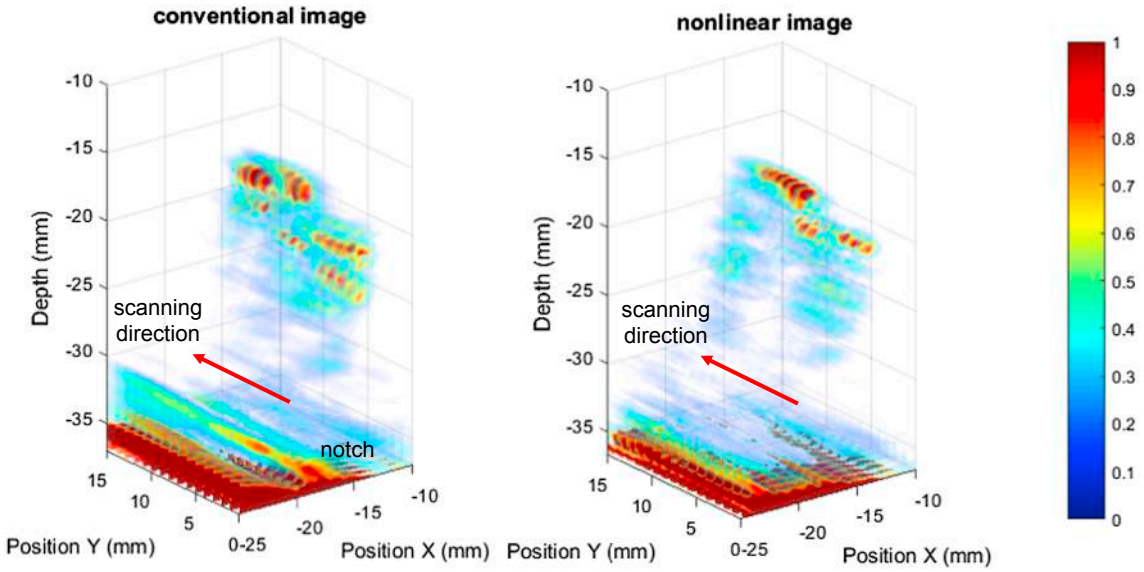

Fig. 8. [Mechanical fatigue crack specimen] 3D scans of the crack along the Y axis using (a) conventional and (b) FAD methods. Step = 1 mm. Normalization of the conventional (i.e. FAD) images is performed by dividing the amplitude of each pixel in the image by the average of the maximum values found in the conventional (i.e. FAD) images among the 16 slices at the crack location (between −12 mm and −25 mm in depth, where 0 mm corresponds to the probe's position).

surprising thing is the shadow that we can observe in the FAD image, behind the crack. The shadow is in the direction of the ultrasonic beam. This pseudo-enhancement of the crack is maybe due to nonlinear propagation after the ultrasound beam crossed the crack [22]. This artifact should be taken into account for future development of FAD method.

4. Conclusion

Fundamental wave amplitude difference (FAD) imaging was compared to the conventional delay-and-sum imaging technique which is still widely used in the industry. The results show that FAD provides a better contrast between the background and the partially-closed part of the crack than the conventional imaging methods. In particular, it was easier to disentangle the response of the crack from the background in FAD. This is particularly interesting when the electronic beam steering is along the crack direction (i.e. parallel scan), which is the worst case for conventional ultrasound. However, it is very important to keep in mind that nonlinear and linear scatterers' are often not collocated in

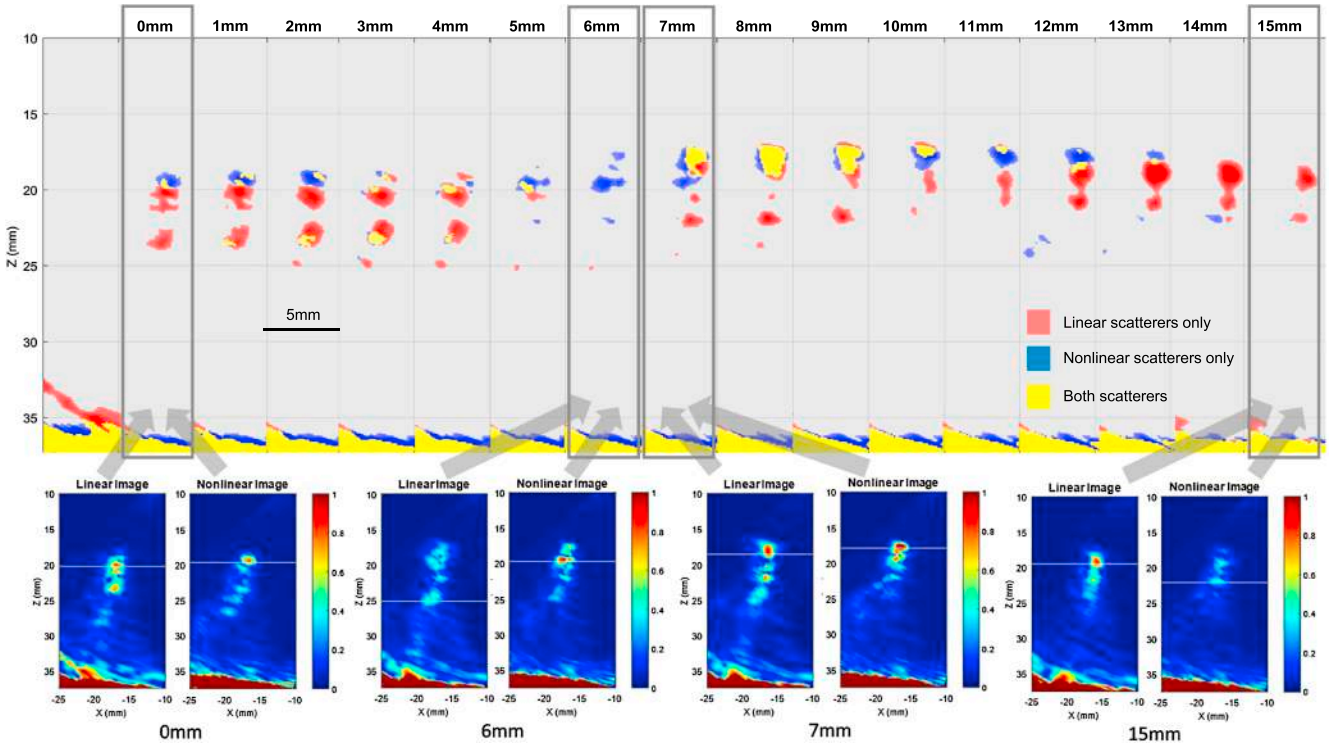

Fig. 9. [Mechanical fatigue crack specimen] Merging of the linear scatterers (i.e. from conventional method) and nonlinear scatterers (i.e. from FAD method) distribution across the crack. Blue color corresponds to the nonlinear response with high energy, red color corresponds to the linear response with high energy and yellow color corresponds to the overlapping of linear and nonlinear responses. Images obtained with both methods at 4 characteristics positions (i.e. 0 mm, 6 mm, 7 mm and 16 mm) are displayed.

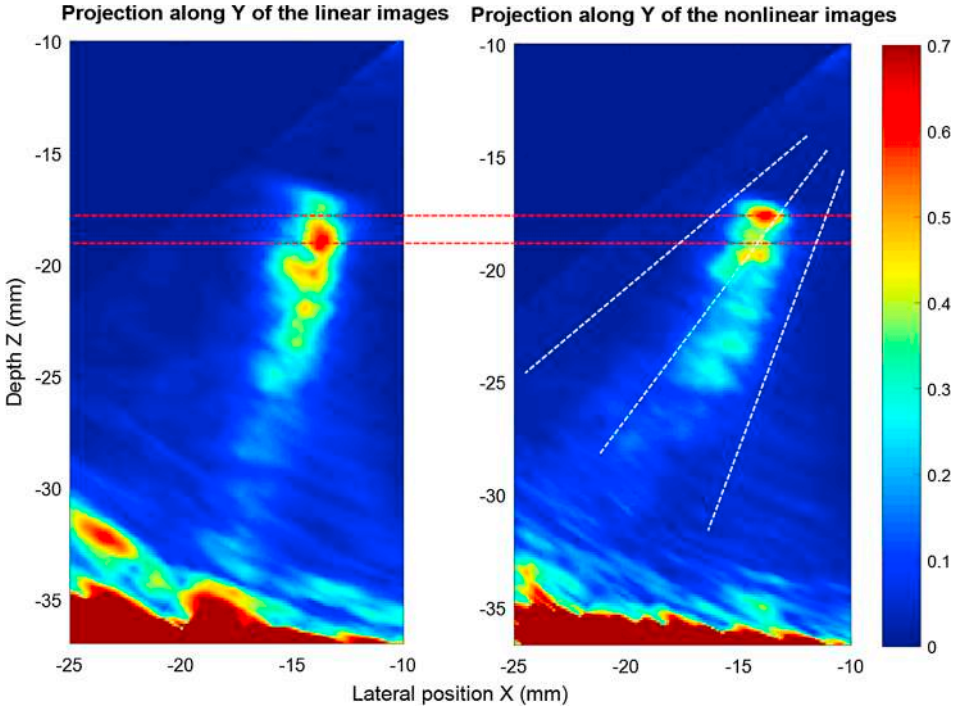

Fig. 10. [Mechanical fatigue crack specimen] Projection of the 16 slices along y-axis. Normalization of the linear (i.e. nonlinear) image is performed with the average maximum value found in the linear (i.e. nonlinear) images among the 16 slices at the crack location (between 12 mm and 25 mm). On the nonlinear image, a shadow behind the crack is observed. The pseudo-enhancement of the crack is maybe due to nonlinear propagation [22]. (Horizontal dotted lines pass by the maximum energy of the crack for each image; inclined dotted lines give indication of the ultrasound beam).

space. Both methods give complementary insight of the whole characteristics of the buried crack. Moreover, it has been shown that the resolution of FAD follows the same rules as the conventional imaging as expected by the fact that both methods share the same bandwidth. It is also worth to notice that all the results were obtained with bulk waves although there are no restrictions on using shear waves instead.

A first attempt of parametric study of the nonlinear elastic behavior of a crack was performed on one specimen. This preliminary result demonstrates the capabilities of FAD to perform quantitative measurements of the nonlinearity suggesting that FAD might be a suitable tool to get a better understanding of the nonlinear mechanism behind the nonlinear response.

FAD involves well known delay-and-sum imaging algorithm such that it is straight forward to implement real-time imaging. In this study, we were able to achieve frame rates between 1 and 5 frames/s depending on the acquisition parameters without optimizing the code. We expect to achieve real-time imaging after implementing the code in C++ with parallel processing on GPUs, making FAD a suitable tool for rapid and wide spread in industry.

Appendix A. Supplementary material

Supplementary data to this article can be found online at https://doi.org/10.1016/j.ultras.2019.02.003.

References

[1] M.-L. Zhu, F.-Z. Xuan, S.-T. Tu, Effect of load ratio on fatigue crack growth in the near-threshold regime: a literature review, and a combined crack closure and driving force approach, Eng. Fract. Mech. 141 (2015) 57–77, https://doi.org/10.1016/j.engfracmech.2015.05.005.

[2] J.D. Frandsen, R.V. Inman, O. Buck, A comparison of acoustic and strain gauge techniques for crack closure, Int. J. Fract. 11 (1975) 345–348.

[3] Y.P. Zheng, R.G. Maev, I.Y. Solodov, Nonlinear acoustic applications for material characterization: a review, Can. J. Phys. 77 (1999) 927–967.

[4] K.Y. Jhang, Nonlinear ultrasonic techniques for nondestructive assessment of micro damage in material: a review, Int. J. Precis. Eng. Manuf. 10 (2009) 123–135.

[5] K.H. Matlack, J.-Y. Kim, L.J. Jacobs, J. Qu, Review of second harmonic generation measurement techniques for material state determination in metals, J. Nondestruct. Eval. 34 (2015) 273, https://doi.org/10.1007/s10921-014-0273-5.

[6] I.Y. Solodov, A.F. Asainov, S.L. Ko, Nonlinear saw reflection – experimental-evidence and NDE applications, Ultrasonics 31 (1993) 91–96.

[7] A.J. Croxford, P.D. Wilcox, B.W. Drinkwater, P.B. Nagy, The use of non-collinear mixing for nonlinear ultrasonic detection of plasticity and fatigue, J. Acoust. Soc. Am. 126 (2009), https://doi.org/10.1121/1.3231451 EL117–22.

[8] Y. Ohara, T. Mihara, R. Sasaki, T. Ogata, S. Yamamoto, Y. Kishimoto, et al., Imaging of closed cracks using nonlinear response of elastic waves at subharmonic frequency, Appl. Phys. Lett. 90 (2007) 011902.

[9] Y. Ohara, Y. Shintaku, S. Horinouchi, M. Ikeuchi, K. Yamanaka, Enhancement of selectivity in nonlinear ultrasonic imaging of closed cracks using amplitude difference phased array, Jpn. J. Appl. Phys. 51 (2012) 07GB18, https://doi.org/10.1143/JJAP.51.07GB18.

[10] M. Ikeuchi, K. Jinno, Y. Ohara, K. Yamanaka, Improvement of closed crack selectivity in nonlinear ultrasonic imaging using fundamental wave amplitude difference, Jpn. J. Appl. Phys. 52 (2013) 07HC08, https://doi.org/10.7567/JJAP.52.07HC08.

[11] S. Haupert, G. Renaud, A. Schumm, Ultrasonic imaging of nonlinear scatterers buried in a medium, NDT E Int. 87 (2017) 1–6, https://doi.org/10.1016/j.ndteint.2016.12.010.

[12] J.N. Potter, A.J. Croxford, P.D. Wilcox, Nonlinear ultrasonic phased array imaging, Phys. Rev. Lett. 113 (2014) 144301, https://doi.org/10.1103/PhysRevLett.113.144301.

[13] J. Cheng, J.N. Potter, B.W. Drinkwater, The parallel-sequential field subtraction technique for coherent nonlinear ultrasonic imaging, Smart Mater. Struct. 27 (2018) 065002.

[14] Y. Ohara, T. Mihara, K. Yamanaka, Effect of adhesion force between crack planes on subharmonic and DC responses in nonlinear ultrasound, Ultrasonics 44 (2006) 194–199.

[15] Y. Ohara, S. Yamamoto, T. Mihara, K. Yamanaka, Ultrasonic evaluation of closed cracks using subharmonic phased array, Jpn. J. Appl. Phys. 47 (2008) 3908.

[16] R.A. Guyer, P.A. Johnson, Nonlinear Mesoscopic Elasticity: The Complex Behaviour of Rocks, Soil, Concrete, Wiley-VCH, Weinheim, 2009.

[17] M. Kemppainen, I. Virkkunen, J. Pitkänen, R. Paussu, H. Hänninen, Advanced flaw production method for in-service inspection qualification mock-ups, Nucl. Eng. Des. 224 (2003) 105–117, https://doi.org/10.1016/S0029-5493(03)00078-5.

[18] L. Landau, E. Lifshitz, J. Sykes, W. Reid, E. Dill, Theory of elasticity: vol. 7 of course of theoretical physics, Phys. Today 13 (1960) 44.

[19] D.L. Miller, Ultrasonic detection of resonant cavitation bubbles in a flow tube by their second-harmonic emissions, Ultrasonics 19 (1981) 217–224.

[20] V. Tournat, V. Zaitsev, V. Gusev, V. Nazarov, P. Béquin, B. Castagnède, Probing weak forces in granular media through nonlinear dynamic dilatancy: clapping contacts and polarization anisotropy, Phys. Rev. Lett. 92 (2004) 085502, https://doi.org/10.1103/PhysRevLett.92.085502.

[21] K.L. Johnson, Contact Mechanics, Cambridge University Press, Cambridge, UK, 1985.

[22] G. Renaud, J.G. Bosch, G.L. ten Kate, V. Shamdasani, R. Entrekin, N. de Jong, et al., Counter-propagating wave interaction for contrast-enhanced ultrasound imaging, Phys. Med. Biol. 57 (2012) L9, https://doi.org/10.1088/0031-9155/57/21/L9.